

See discussions, stats, and author profiles for this publication at: <https://www.researchgate.net/publication/231731854>

# Structure, Vibrational Spectra, and DFT and ab Initio Calculations of Silacyclobutanes

ARTICLE in ORGANOMETALLICS · JULY 2008

Impact Factor: 4.13 · DOI: 10.1021/om800296w

---

CITATIONS

15

---

READS

17

## 2 AUTHORS:



**Abdulaziz Al-Saadi**

King Fahd University of Petroleum and Min...

79 PUBLICATIONS 322 CITATIONS

SEE PROFILE



**Jaan Laane**

Texas A&M University

265 PUBLICATIONS 4,253 CITATIONS

SEE PROFILE

# Structure, Vibrational Spectra, and DFT and *ab Initio* Calculations of Silacyclobutanes

Abdulaziz A. Al-Saadi<sup>†,‡</sup> and Jaan Laane<sup>\*,†</sup>

Department of Chemistry, Texas A&M University, College Station, Texas 77843-3255, and Chemistry Department, King Fahd University of Petroleum and Minerals, Dhahran 31261, Saudi Arabia

Received April 2, 2008

*Ab initio* calculations have been carried out for silacyclobutane (SCB) and its 1,1-difluoro and 1,1-dichloro derivatives in order to compute the structures and dihedral angles of puckering for these molecules. For SCB the calculated dihedral angle of 35° agrees nicely with the 36° value obtained from far-infrared work. The calculated angles of 29° and 31° for the fluoro and chloro derivatives, respectively, can be compared to electron diffraction results of 25° and 26°. The zero-point-corrected barriers calculated using the MP2/cc-pVTZ level of theory were 523 (as compared to 440 cm<sup>-1</sup> experimental), 186, and 433 cm<sup>-1</sup> for SCB and its fluoro and chloro derivatives, respectively. Calculated structural changes in the dihalo derivatives can be ascribed to the high electronegativity of the halogen atoms. High-level DFT computations were also carried out in order to calculate the infrared and Raman spectra of these three molecules as well as the SCB 1,1-*d*<sub>2</sub> isotopomer. The agreement between experimental and calculated spectra is remarkably good for all four molecules. The predicted frequencies and intensities were utilized to reassign several of the weaker spectral bands and also to characterize the 1130 cm<sup>-1</sup> signature band present in the infrared spectra of all silacyclobutanes. This arises from the α-CH<sub>2</sub> in-phase wagging vibration, which is very much affected by the neighboring silicon atom. The DFT calculations also demonstrated that two of the wagging and twisting motions of the CH<sub>2</sub> group next to the silicon atom have frequencies much lower than in typical organic molecules. This work also provides frequency ranges that can be expected for the six vibrations of SiX<sub>2</sub> groups (X = H, D, F, Cl) in organosilanes.

## Introduction

Silacyclobutane derivatives were first synthesized by Sommer and Baum<sup>1</sup> in 1954, and in 1963 Vdovin and co-workers<sup>2</sup> synthesized 1,1-dichloro-1-silacyclobutane. The preparation of silacyclobutane (SCB) itself and its 1,1-difluoro derivative were first reported in 1967 by Laane,<sup>3</sup> who also presented the characteristic infrared spectral bands and NMR spectra for these molecules. The following year Laane and Lord<sup>4</sup> published the far-infrared spectrum of SCB and its 1,1-*d*<sub>2</sub> isotopomer and determined the one-dimensional ring-puckering potential energy function for this molecular system. From the potential energy function they determined that the molecule is bent with a dihedral angle of 36° and has a barrier to planarity of 440 cm<sup>-1</sup> (5.26 kJ/mol). Later electron diffraction work,<sup>5,6</sup> which averages structures over the different vibrational states, estimated the dihedral angle to be 34°. For the dihalo derivatives, electron

diffraction studies reported dihedral angles of bending of 25° for the difluoride<sup>7</sup> and 26° to 32° for the dichloride.<sup>8–11</sup> A comprehensive study of the vibrational spectra and force constant calculations of SCB and its 1,1-*d*<sub>2</sub> isotopomer as well as the two dihalo derivatives was published by Laane<sup>12</sup> in 1970. This work not only provided complete vibrational assignments, but also demonstrated that several previously accepted SiX<sub>2</sub> group frequencies<sup>13,14</sup> could be significantly shifted by vibrational coupling with other modes. The study also proposed that the characteristic and intense infrared absorption frequency near 1130 cm<sup>-1</sup> for these molecules was the CH<sub>2</sub> wagging at the carbon atoms adjacent to the silicon atom in the ring.

Several *ab initio* investigations of the structures, energetic behavior, and vibrational frequencies of SCB and its derivatives have also been published.<sup>6,7,11,15–23</sup> Molecular mechanics<sup>24–26</sup>

\* Corresponding author. E-mail: laane@mail.chem.tamu.edu.

<sup>†</sup> Texas A&M University.

<sup>‡</sup> King Fahd University of Petroleum and Minerals.

- (1) Sommer, L. H.; Baum, G. A. *J. Am. Chem. Soc.* **1954**, *76*, 5002.
- (2) Vdovin, V. M.; Nametkin, N. S.; Grinberg, P. L. *Dokl. Akad. Nauk SSSR* **1963**, *150*, 799.
- (3) Laane, J. *J. Am. Chem. Soc.* **1967**, *89*, 1144.
- (4) Laane, J.; Lord, R. C. *J. Chem. Phys.* **1968**, *48*, 1508.
- (5) Mastryukov, V. S.; Dorofeeva, O. V.; Vilkov, L. V.; Cyvin, B. N.; Cyvin, S. J. *Zh. Strukt. Khim.* **1975**, *16*, 438.
- (6) Novikov, V. P.; Dakkouri, M.; Vilkov, L. V. *J. Mol. Struct.* **2006**, *800*, 146.
- (7) Rempfer, B.; Pfaffertott, G.; Oberhammer, H.; Auner, N.; Boggs, J. E. *Acta Chem. Scand.* **1988**, *A42*, 352.
- (8) Vilkov, L. V.; mastryukov, V. S.; Baurova, Y. V.; Vdovin, V. M. *Dokl. Akad. Nauk SSSR* **1967**, *117*, 1084.
- (9) Aleksanya, V. T.; Kuz'yants, G. M.; Vdovin, V. M.; Grinberg, P. L.; Kuz'min, O. V. *Zh. Strukt. Khim.* **1969**, *10*, 397.

(10) Cyvin, B. N.; Cyvin, S. J.; Strelkov, S. A.; Mastryukov, V. S.; Vilkov, L. V.; Golubinskii, A. V. *J. Mol. Struct.* **1986**, *144*, 385.

(11) Novikov, V. P.; Tarasenko, S. A.; Samdal, S.; Vilkov, L. V. *J. Mol. Struct.* **1998**, *445*, 207.

(12) Laane, J. *Spectrochim. Acta* **1970**, *26A*, 517.

(13) Smith, A. L. *Spectrochim. Acta* **1960**, *16*, 87.

(14) Smith, A. L. *Spectrochim. Acta* **1963**, *19*, 849.

(15) Boatz, J. A.; Gordon, M. S.; Hildebrandt, R. L. *J. Am. Chem. Soc.* **1988**, *110*, 352.

(16) Seidl, E. T.; Grev, R. S.; Schaefer, H. F., III *J. Am. Chem. Soc.* **1992**, *114*, 3643.

(17) Skancke, P. N. *J. Phys. Chem.* **1994**, *98*, 3154.

(18) Mastryukov, V. S.; Boggs, J. E. *J. Mol. Struct. (THEOCHEM)* **1995**, *338*, 235.

(19) Fangstrom, T.; Lunell, S.; Engels, B.; Eriksson, L. A.; Shiotani, M.; Komaguchi, K. *J. Chem. Phys.* **1997**, *107*, 297.

(20) Gordon, M. S.; Barton, T. J.; Nakano, H. *J. Am. Chem. Soc.* **1997**, *119*, 11966.

(21) Khabashesku, V. N.; Kudin, K. N.; Margrave, J. L. *Russ. Chem. Bull., Int. Ed.* **2001**, *50*, 20.

studies on the structure of SCB have also been carried out. The MM2 method<sup>24</sup> predicted the barrier to inversion to be 462 cm<sup>-1</sup> and a puckering angle of 32°, while the extended MM3 method<sup>25,26</sup> predicted a barrier of 395 cm<sup>-1</sup>.

The vibrational frequencies of SCB have been previously computed using the restricted Hartree–Fock self-consistent-field (HF-SCF) calculations<sup>16</sup> and density functional theory (DFT-B3LYP) utilizing the 6-311G(d,p) basis set.<sup>21</sup> In these two studies the vibrational assignments were made on the basis of the unscaled frequencies and the infrared intensities with comparison to the previously reported vibrational spectral data.<sup>12</sup>

Recently a combined gas-phase electron diffraction study and *ab initio* calculation on the structure of SCB has been reported by Navikov, Dakkouri, and Vilkov<sup>6</sup> (hereafter abbreviated as NDV). In the NDV work, Hartree–Fock, second-order Møller–Plesset, and DFT-B3LYP theories were implemented using different basis sets. From their work it was clear that the effect of including electron correlations produces better predictions of structures and barriers. Comparisons between the present work and NDV will be presented later.

Now, four decades after our initial structural and spectroscopic work, equipped with new computational tools, we will examine again the structures of these molecules using very high level *ab initio* calculations, and we will investigate how well density functional theory (DFT) calculations do in predicting the vibrational frequencies of all four molecules. These methods are known to work well for hydrocarbons, but far fewer studies have been carried out for organosilanes. We recently reported our results on the 1,3-disilacyclobutane (DSCB) ring system<sup>27</sup> and showed that cyclic organosilanes possess many unusual structural and spectroscopic features.

### Theoretical Calculations

SCB has *C<sub>s</sub>* symmetry for its puckered structure but closely follows *C<sub>2v</sub>* planar structure selection rules since it is a nonrigid molecule that can vibrate back and forth through its planar structure. The structures, the inversion barriers, and the vibrational frequencies of SCB, 1,1-difluorosilacyclobutane, and 1,1-dichlorosilacyclobutane were studied in this work using density functional theory (DFT) with the B3LYP hybrid functional and second-order Møller–Plesset (MP2) calculations using the Gaussian 03 program.<sup>28</sup> The vibra-

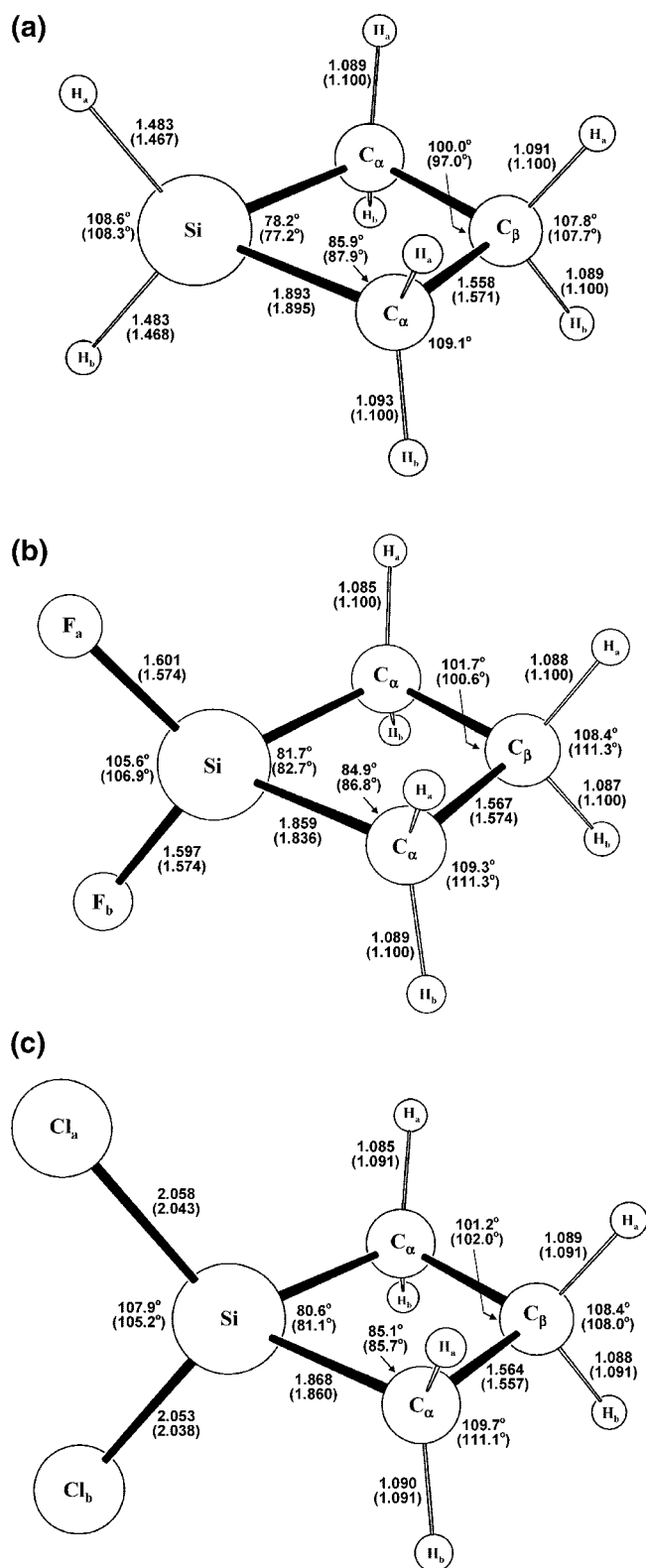


**Figure 1.** Structures and atom labels for (a) silacyclobutane, (b) 1,1-difluorosilacyclobutane, and (c) 1,1-dichlorosilacyclobutane. The values in parentheses are from electron diffraction experiments.

tional frequencies of silacyclobutane-1,1-*d*<sub>2</sub> were also calculated. Different basis sets including the cc-pVTZ (triple- $\zeta$ ) were used to compute the geometry of the planar and puckered structures of SCB and the structures of the dihalo derivatives. The barriers to planarity of silacyclobutane and the difluoro and dichloro derivatives were calculated and were zero-point corrected. The vibrational frequencies, infrared and Raman band intensities, and depolarization ratios

(22) Damrauer, R.; Crowell, A. J.; Craig, C. F. *J. Am. Chem. Soc.* **2003**, *125*, 10759.

(23) Freeman, F.; Fang, C.; Shaiyuan, B. A. *Int. J. Quantum Chem.* **2004**, *100*, 720.

(24) Rosas, R. L.; Cooper, C.; Laane, J. *J. Phys. Chem.* **1990**, *94*, 1830.

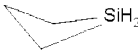


(25) Frierson, M. R.; Imam, M. R.; Zalkow, V. B.; Allinger, N. L. *J. Org. Chem.* **1988**, *53*, 5248.

(26) Chen, K.; Allinger, N. L. *J. Phys. Org. Chem.* **1997**, *10*, 697.

(27) Rishard, M. Z. M.; Irwin, R. M.; Laane, J. *J. Phys. Chem. A* **2007**, *111*, 825.

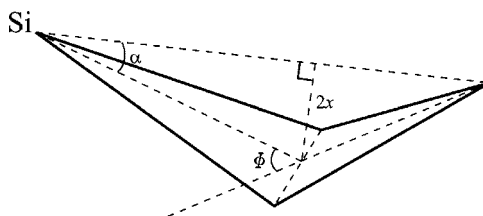
(28) Frisch, M. J.; Trucks, G. W.; Schlegel, H. B.; Scuseria, G. E.; Robb, M. A.; Cheeseman, J. R.; Montgomery, J. A., Jr.; Vreven, T.; Kudin, K. N.; Burant, J. C.; Millam, J. M.; Iyengar, S. S.; Tomasi, J.; Barone, V.; Mennucci, B.; Cossi, M.; Scalmani, G.; Rega, N.; Petersson, G. A.; Nakatsuji, H.; Hada, M.; Ehara, M.; Toyota, K.; Fukuda, R.; Hasegawa, J.; Ishida, M.; Nakajima, T.; Honda, Y.; Kitao, O.; Nakai, H.; Klene, M.; Li, X.; Knox, J. E.; Hratchian, H. P.; Cross, J. B.; Bakken, V.; Adamo, C.; Jaramillo, J.; Gomperts, R.; Stratmann, R. E.; Yazyev, O.; Austin, A. J.; Cammi, R.; Pomelli, C.; Ochterski, J. W.; Ayala, P. Y.; Morokuma, K.; Voth, G. A.; Salvador, P.; Dannenberg, J. J.; Zakrzewski, V. G.; Dapprich, S.; Daniels, A. D.; Strain, M. C.; Farkas, O.; Malick, D. K.; Rabuck, A. D.; Raghavachari, K.; Foresman, J. B.; Ortiz, J. V.; Cui, Q.; Baboul, A. G.; Clifford, S.; Cioslowski, J.; Stefanov, B. B.; Liu, G.; Liashenko, A.; Piskorz, P.; Komaromi, I.; Martin, R. L.; Fox, D. J.; Keith, T.; Al-Laham, M. A.; Peng, C. Y.; Nanayakkara, A.; Challacombe, M.; Gill, P. M. W.; Johnson, B.; Chen, W.; Wong, M. W.; Gonzalez, C.; Pople, J. A. *Gaussian 03, Revision C.02*; Gaussian, Inc.: Wallingford, CT, 2004.

**Table 1.** Calculated Structural Parameters for Silacyclobutane and 1,1-Difluoro- and 1,1-Dichlorosilacyclobutanes from the MP2/cc-pVTZ Level of Theory Compared with Different Experiments

						
	Calc.	ED <sup>a</sup>	Calc.	ED <sup>b</sup>	Calc.	ED <sup>c</sup>
Bond lengths (Å)						
Si—C	1.893	1.895	1.859	1.836	1.868	1.860
C—C	1.558	1.571	1.567	1.574	1.564	1.557
C <sub>α</sub> —H <sub>a</sub>	1.086	1.100	1.085	1.099	1.085	1.091
C <sub>α</sub> —H <sub>b</sub>	1.090	1.100	1.089	1.099	1.090	1.091
C <sub>β</sub> —H <sub>a</sub>	1.091	1.100	1.088	1.099	1.089	1.091
C <sub>β</sub> —H <sub>b</sub>	1.089	1.100	1.087	1.099	1.088	1.091
Si—X <sub>a</sub>	1.483	1.467	1.601	1.574	2.058	2.043
Si—X <sub>b</sub>	1.483	1.468	1.597	1.574	2.053	2.038
Bond angles (°)						
∠CSiC	78.2	77.2	81.7	82.7	80.6	81.1
∠SiCC	85.9	87.9	84.9	86.8	85.1	85.7
∠CCC	100.0	97.0	101.7	100.6	101.2	102.0
∠XSiX	108.6	108.3	105.6	106.9	107.9	105.2
∠HC <sub>α</sub> H	109.1		109.3	111.3	109.7	125.7
∠HC <sub>β</sub> H	107.8	107.7	108.4	111.3	108.4	108.0
∠C <sub>β</sub> C <sub>α</sub> H <sub>a</sub>	116.6	118.4	116.0		116.6	105.3
∠C <sub>β</sub> C <sub>α</sub> H <sub>b</sub>	110.1	112.3	110.6		110.7	100.9
∠C <sub>α</sub> C <sub>β</sub> H <sub>a</sub>	109.5		109.7		109.8	110.0
∠C <sub>α</sub> C <sub>β</sub> H <sub>b</sub>	114.9		113.6		113.7	113.4
∠SiCH <sub>a</sub>	122.6	123.5	122.1		121.7	118.9
∠SiCH <sub>b</sub>	110.5	111.9	111.8		110.9	109.7
∠CSiX <sub>a</sub>	112.3		113.6		112.4	114.7
∠CSiX <sub>b</sub>	121.4		120.7		120.8	120.2
Φ <sup>d</sup>	34.5	33.5 (ED) 36 (FIR) <sup>e</sup>	28.7	25	31.1	25.9

<sup>a</sup> Ref 6. <sup>b</sup> Ref 7. <sup>c</sup> Ref 11. <sup>d</sup> Puckering angle (see definition in Table 2). <sup>e</sup> Refs 4, 24.**Table 2.** Puckering Coordinates, Theoretical Potential Energy Function Parameters, and Rotational Constants for Silacyclobutane Based on *ab Initio* Calculations<sup>a</sup>

method	puckering angle $\phi$ (deg)	$x$ (Å)	$V(\text{cm}^{-1}) = ax^4 - bx^2$		rotational constants ( $\text{cm}^{-1}$ )
			$a$ (Å <sup>-4</sup> )	$b$ (Å <sup>-2</sup> )	
MP2/6-31G	30.2	0.182	$3.01 \times 10^5$	$19.84 \times 10^5$	0.2891, 0.1341, 0.1952
MP2/6-31+G(d)	32.9	0.162	$3.55 \times 10^5$	$18.63 \times 10^5$	0.2954, 0.1414, 0.2073
MP2/6-311++G(d,p)	34.2	0.173	$3.69 \times 10^5$	$22.11 \times 10^5$	0.2957, 0.1422, 0.2082
MP2/cc-pVTZ	34.5	0.181	$3.57 \times 10^5$	$23.32 \times 10^5$	0.2963, 0.1427, 0.2091
B3LYP/cc-pVTZ	27.7	0.144	$3.87 \times 10^5$	$16.12 \times 10^5$	0.2945, 0.1395, 0.2068
experimental	36 <sup>b</sup>	0.184	$3.85 \times 10^5$	$26.06 \times 10^3$	0.2941, 0.1416, 0.2098 <sup>c</sup>

<sup>a</sup> Definitions of the parameters  $\phi$  and  $x$  are shown below:<sup>b</sup> Refs 4, 24. <sup>c</sup> Refs 29.

for the four molecules were calculated using density functional theory (B3LYP/cc-pVTZ) and by implementing the appropriate scaling factors.

### Molecular Structure

Figure 1 shows the structures and geometrical parameters calculated for silacyclobutane, 1,1-difluorosilacyclobutane, and 1,1-dichlorosilacyclobutane. The bond lengths, bond angles, and puckering angles for the puckered  $C_s$  and planar  $C_{2v}$  structure

of the three molecules are given in more detail in Table 1 and are compared to experimental structures reported in the literature. Except for the dihedral angle of puckering, which was very accurately determined from the potential energy minimum in the far-infrared study,<sup>4</sup> the results are from electron diffraction work that present the geometrical parameters averaged over all of the occupied vibrational quantum states. Since these molecules have a large number of low-energy vibrational levels, the electron diffraction values can be expected to disagree somewhat from the

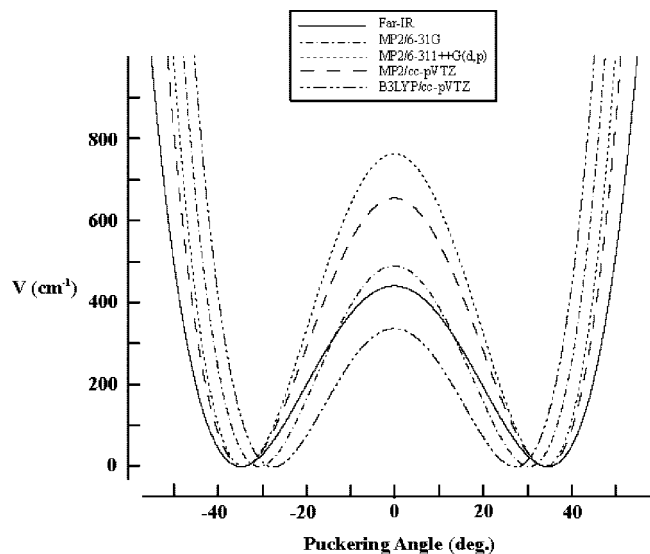


**Figure 2.** Puckering-angle potential energy functions for silacyclobutane from different levels of theory compared to far-infrared experimental values.

**Table 3. Barrier to Planarity and Puckering Angle for Silacyclobutane from Different Experimental and *ab Initio* Method**

method	barrier (cm <sup>-1</sup> )	zero-point-corrected barrier (cm <sup>-1</sup> )	puckering angle (deg)
MP2/6-31G	489	343	30.2
MP2/6-31+G(d)	663	514	32.9
MP2/6-311++G(d,p)	762	559	34.2
MP2/6-311++G(2d,p)	712	512	34.3
MP2/6-311+G(df,pd) <sup>a</sup>	786		35.0
MP2/cc-pVTZ	654	523	34.5
B3LYP/6-31G	113	49	22.9
B3LYP/6-31+G(d)	240	157	27.0
B3LYP/6-311++G(d,p)	243	160	27.2
B3LYP/6-311++G(2d,p)	257	169	27.4
B3LYP/6-311++G(df,pd) <sup>a</sup>	276		27.9
B3LYP/cc-pVTZ	336	248	27.7
far-infrared <sup>b</sup>		440	36
microwave <sup>c</sup>			28
ED <sup>a,d</sup>			34

<sup>a</sup> Ref 6. <sup>b</sup> Refs 4, 24. <sup>c</sup> Ref 29. <sup>d</sup> Ref 5.

*ab initio* results for the lowest energy structure in its ground vibrational state. In the previous microwave work,<sup>29</sup> which utilized

**Table 4. Barriers to Planarity and Puckering Angles for 1,1-Difluoro-1-silacyclobutane and 1,1-Dichloro-1-silacyclobutane from Different Methods of Calculations**

method	barrier (cm <sup>-1</sup> )	zero-point-corrected barrier (cm <sup>-1</sup> )	puckering angle (deg)
1,1-Difluoro-1-silacyclobutane			
MP2/6-31G	279	135	25.2
MP2/6-311++G(d,p)	338	181	28.1
MP2/cc-pVTZ	297	186	28.7
B3LYP/cc-pVTZ	58		19.4
ED <sup>a</sup>	418		25
1,1-Dichloro-1-silacyclobutane			
MP2/6-31G	388	246	27.8
MP2/6-311++G(d,p)	676	473	30.6
MP2/cc-pVTZ	453	344	31.1
B3LYP/cc-pVTZ	96		22.6
ED (Vilkov) <sup>b</sup>			30
ED (Cyvin) <sup>c</sup>			31.7
ED (Novikov) <sup>d</sup>			25.9

<sup>a</sup> Ref 7. <sup>b</sup> Ref 4. <sup>c</sup> Ref 8. <sup>d</sup> ref 11.

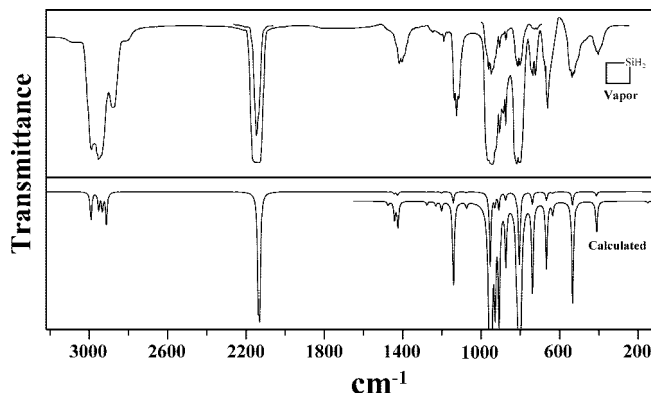


**Figure 3.** Vapor-phase (from ref 38) and calculated (DFT-B3LYP/cc-pVTZ) infrared spectra of silacyclobutane.

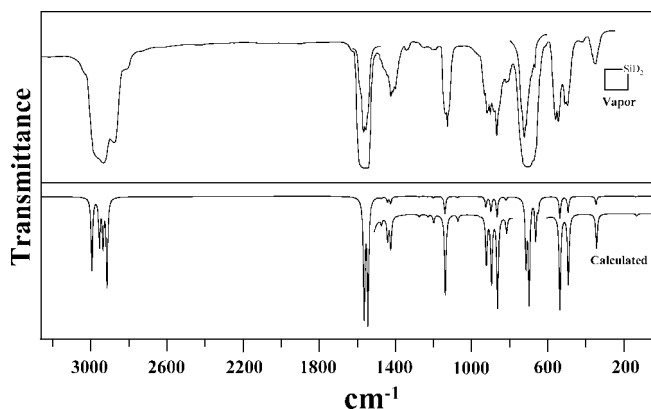


**Figure 4.** Vapor-phase (from ref 38) and calculated (DFT-B3LYP/cc-pVTZ) infrared spectra of silacyclobutane-1,1-d<sub>2</sub>.

the same sample and potential energy function as the far-infrared study,<sup>4</sup> the geometrical parameters were not determined, but the rotational constants were given for the lowest vibrational energy state. Table 2 shows how well the experimental microwave values agree with those calculated from the structures predicted using the different basis sets. All of the MP2 calculations except the simplest calculation (MP2/6-31G) do a good job of calculating the rotational constants, and the triple- $\zeta$  (MP2/cc-pVTZ) does a remarkable job, as the average difference between the experimental and computed values is only 0.6%. In other words, the *ab initio* calculation at this very high level essentially does a perfect job of predicting the actual molecular structure. As also shown in Table 2, and as will be discussed below, this level of computation also does an excellent job of simulating the potential energy changes associated with the puckering of this four-membered ring.

Examination of the structural differences between the three molecules in Figure 1 and Table 1 shows several trends that primarily are due to the electronegativity differences between hydrogen, fluorine, and chlorine. The Si–X bond distance, of course, depends primarily on the size of the X atom, and the values increase from 1.483 for X = H, to 1.597 (F), to 2.053 Å (Cl); these values are quite typical for silanes and silicon halides. The Si–C bond distance, however, decreases significantly with the electronegativity of the X atom with values of 1.893, 1.868, and 1.859 Å for X = H, Cl, and F, respectively. As expected, a much smaller effect is seen on the C–C bond, which increases slightly with electronegativity of the X atom (1.558, 1.564, and 1.567 Å, respectively). The interior and exterior angles at the



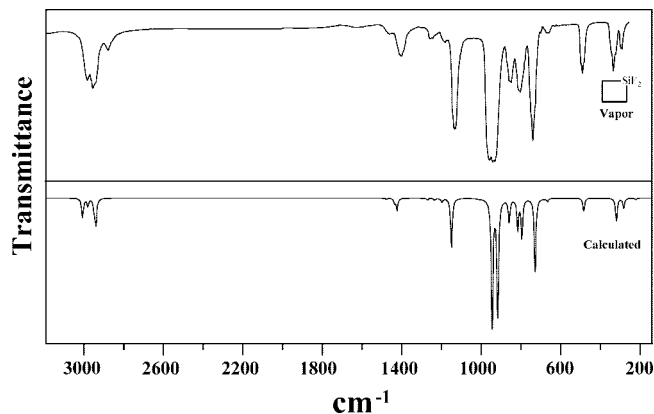


**Figure 5.** Vapor-phase (from ref 38) and calculated (DFT-B3LYP/cc-pVTZ) infrared spectra of 1,1-difluorosilacyclobutane.

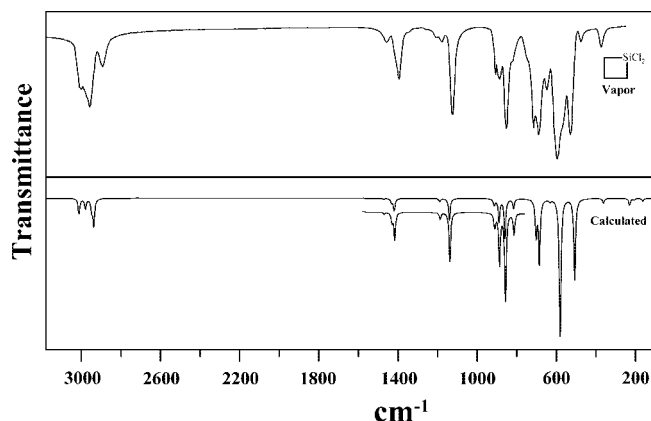


**Figure 6.** Vapor-phase (from ref 38) and calculated (DFT-B3LYP/cc-pVTZ) infrared spectra of 1,1-dichlorosilacyclobutane.

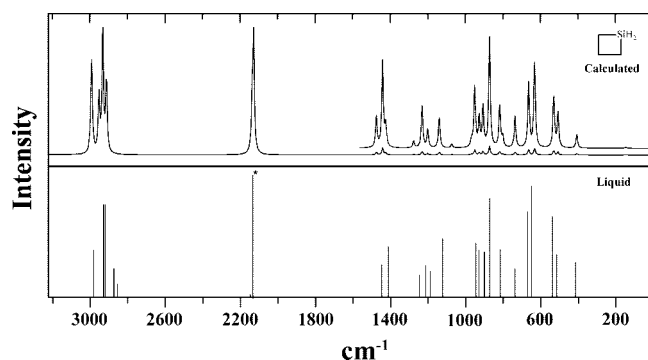


**Figure 7.** Calculated (DFT-B3LYP/cc-pVTZ) Raman spectra for silacyclobutane compared with the line spectra of the frequencies and intensities of the liquid-phase Raman spectra reported in refs 12 and 38. Lines marked with (\*) indicate peaks with greater intensities than shown.

silicon atom also show significant changes with electronegativity. The XSiX angle decreases with electronegativity from 108.6° (H), to 107.9° (Cl), to 105.6° (F), while the CSiC angle increases from 78.2° (H), to 80.6° (Cl), to 81.7° (F). As can be seen, the experimental electron diffraction values agree well but not perfectly with the calculated ones.

The previous far-infrared work<sup>4</sup> together with the refined reduced mass calculation<sup>24</sup> very accurately determined the ring-puckering potential energy for silacyclobutane as a function of the degree of bending as measured by its puckering coordinate or dihedral angle. In the present work we have utilized different basis sets for the MP2 and B3LYP calculations and examined

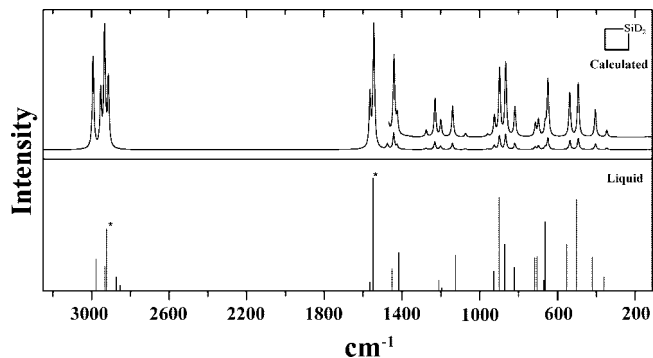


**Figure 8.** Calculated (DFT-B3LYP/cc-pVTZ) Raman spectra for silacyclobutane-1,1-*d*<sub>2</sub> compared with the line spectra of the frequencies and intensities of the liquid-phase Raman spectra reported in refs 12 and 38. Lines marked with (\*) indicate peaks with greater intensities than shown.

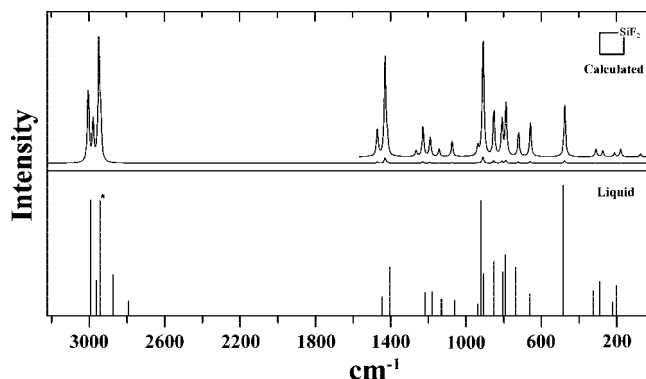


**Figure 9.** Calculated (DFT-B3LYP/cc-pVTZ) Raman spectra for 1,1-difluorosilacyclobutane compared with the line spectra of the frequencies and intensities of the liquid-phase Raman spectra reported in refs 12 and 38. Lines marked with (\*) indicate peaks with greater intensities than shown.

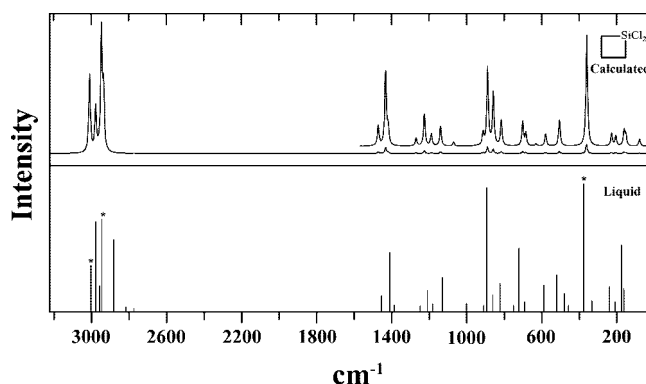


**Figure 10.** Calculated (DFT-B3LYP/cc-pVTZ) Raman spectra for 1,1-dichlorosilacyclobutane compared with the line spectra of the frequencies and intensities of the liquid-phase Raman spectra reported in refs 12 and 38. Lines marked with (\*) indicate peaks with greater intensities than shown.

how well these do for reproducing the experimental results. Table 2 and Figure 2 compare these results. The experimental potential energy function has the form  $V = ax^4 - bx^2$  where  $x$  is the ring-puckering coordinate, which measures the degree of nonplanarity of the molecule. As is evident, the *ab initio* MP2/cc-pVTZ triple- $\zeta$  calculation does an excellent job of reproducing the experimental result, and its calculated energy minimum at 34.5° agrees favorably with the experimental value of 36°. The B3LYP/cc-pVTZ calculation even at the triple- $\zeta$  level does

Table 5. Vibrational Spectra of Silacyclobutane

description	experimental <sup>a</sup>			calculated DFT-B3LYP					
			Raman <sup>b</sup>	<i>C<sub>s</sub></i>			<i>C<sub>2v</sub></i>		
	IR <sup>b</sup>			scaled	intensity	dep. ratio	scaled	intensity	dep. ratio
A <sub>1</sub> , A'	$\nu_1$ $\beta$ -CH <sub>2</sub> sym. str.	2935 m	2927 (756)	p	2914 (32, 602)	0.2	2925 (275,410)	0.3	
	$\nu_2$ $\alpha$ -CH <sub>2</sub> sym. str. (i.p.)	2873 m	2858 (90)	p	2933 (1,989)	0.2	2948 (37,1284)	0.3	
	$\nu_3$ SiH <sub>2</sub> sym. str.	2145 vvv	2137 (1000)	p	2130 (100, 1000)	0.1	2127 (1000,1000)	0.1	
	$\nu_4$ $\alpha$ -CH <sub>2</sub> deform. (i.p.)	1422* m	1414* (67)	d	1443 (2,56)	0.7	1435 (3,66)	0.7	
	$\nu_5$ $\beta$ -CH <sub>2</sub> deform.	1458* vvw	1450* (29)	d	1476 (1,20)	0.7	1471 (4,15)	0.7	
	$\nu_6$ $\alpha$ -CH <sub>2</sub> wag. (i.p.)	1127 s	1123 (84)	p	1141 (11,20)	0.2	1137 (113,18)	0.1	
	$\nu_7$ SiH <sub>2</sub> deform.	962 vvs	948 (75)	d	952 (73,40)	0.7	954 (760,39)	0.7	
	$\nu_8$ C—C sym. str.	877* s	876* (169)	p	873 (7,73)	0.1	874 (1,87)	0.1	
	$\nu_9$ Si—C sym. str.		817* (60)	p	819 (4,28)	0.1	763 (0,70)	0.1	
	$\nu_{10}$ ring deform.	532 m	539 (130)	p	531 (13,34)	0.2	507 (86,46)	0.2	
A <sub>2</sub> , A''	$\nu_{11}$ $\alpha$ -CH <sub>2</sub> antisym. str. (o.p.)	2992* vs	2980* (378)	d	2992 (11,410)	0.8	2987 (0,633)	0.8	
	$\nu_{12}$ $\alpha$ -CH <sub>2</sub> twist. (o.p.)				969 (0,5)	0.8	976 (0,3)	0.8	
	$\nu_{13}$ $\beta$ -CH <sub>2</sub> twist.	1211* vw	1214* (28)	d	1232 (1,27)	0.8	1238 (0,18)	0.8	
	$\nu_{14}$ $\alpha$ -CH <sub>2</sub> rock. (o.p.)	736 m	740 (21)	d	737 (11,21)	0.8	751 (0,25)	0.8	
	$\nu_{15}$ SiH <sub>2</sub> twist	514 w	517 (50)	d	508 (1,23)	0.8	484 (0,22)	0.8	
B <sub>1</sub> , A'	$\nu_{16}$ $\alpha$ -CH <sub>2</sub> sym. str. (o.p.)	2888 m	2876 (220)	p	2935 (16,71)	0.8	2945 (260,32)	0.8	
	$\nu_{17}$ $\alpha$ -CH <sub>2</sub> deform. (o.p.)	1401 m			1426 (3,14)	0.8	1426 (48,1)	0.8	
	$\nu_{18}$ $\alpha$ -CH <sub>2</sub> wag (o.p.)				1074 (1,3)	0.8	1102 (1,0)	0.8	
	$\nu_{19}$ $\beta$ -CH <sub>2</sub> wag	1255* vw [sol.]	1250* (7)	d	1277 (1,4)	0.8	1271 (16,9)	0.8	
	$\nu_{20}$ C—C antisym. str.	927 s	932 (60)	d	928 (11,19)	0.8	937 (110,18)	0.8	
B <sub>2</sub> , A''	$\nu_{21}$ Si—C antisym. str.	653 m [sol.]	652 (194)	d	633 (2,56)	0.8	640 (20,55)	0.8	
	$\nu_{22}$ SiH <sub>2</sub> wag	814 vs			803 (71,7)	0.8	799 (886,5)	0.8	
	$\nu_{23}$ $\beta$ -CH <sub>2</sub> antisym. str.	2953* vs			2954 (17,491)	0.4	2957 (33,198)	0.8	
	$\nu_{24}$ $\alpha$ -CH <sub>2</sub> antisym. str. (i.p.)	2992* vs	2980* (378)	d	2994 (16,418)	0.2	2993 (255,163)	0.8	
	$\nu_{25}$ SiH <sub>2</sub> antisym. str.	2145 vvv	2150 w	d	2138 (92,424)	0.7	2132 (984,421)	0.8	
	$\nu_{26}$ $\alpha$ -CH <sub>2</sub> twist. (i.p.)	1191 mw	1191 (16)	d	1202 (1,12)	0.4	1191 (22,9)	0.8	
	$\nu_{27}$ $\alpha$ -CH <sub>2</sub> rock. (i.p.)	906* ms	903 (58)	p	908 (16,26)	0.2	879 (248,5)	0.8	
	$\nu_{28}$ $\beta$ -CH <sub>2</sub> rock	673 ms	671 (141)	p	665 (9,42)	0.1	712 (75,0)	0.8	
	$\nu_{29}$ SiH <sub>2</sub> rock	409 mw	418 (34)	d	409 (4,9)	0.3	427 (81,3)	0.8	
	$\nu_{30}$ ring puckering	158 <sup>c</sup>			147 (0,1)	0.4	<i>i</i> <sup>d</sup>		

<sup>a</sup> Reassigned frequencies are labeled with (\*). <sup>b</sup> Vapor-phase experiments from ref 12, [sol.] = solid state. <sup>c</sup> Ref 4. <sup>d</sup> Imaginary frequencies for the higher energy structure. This also is applied to the notation *i* appearing in Tables 8–10.

a poorer job. However, as we shall see, the B3LYP calculations do better in calculating the vibrational frequencies.

Table 3 compares the calculated barriers to planarity and the dihedral angles of SCB using different basis sets. The basic observation is that the MP2 calculations, even with small basis sets such as 6-31G, do a much better job of predicting the barrier and dihedral angle than do the DFT calculations. Implementing smaller basis sets means there are more constraints in describing the molecular orbitals of the system because of the lower number of basis functions employed in the calculations. In addition, the 6-31G is more limited, as it includes neither diffuse functions nor polarization functions, which are responsible for giving more flexibility to the description of the orbitals involved.<sup>30–33</sup> As noted above, the calculated puckering angle from the triple- $\zeta$  basis set (34.5°) was the closest to the experimental silacyclobutane value. The barriers and puckering angles calculated by the Hartree–Fock and DFT methods were found to be considerably lower than the experimental values for not only the silacyclobutane molecule but also its difluoro and dichloro derivatives (Tables 3 and 4). The underestimation of the inversion barriers and dihedral angles by the DFT method for different cyclic molecules as compared to experimental values, including the ones being studied in this work, has been noted in several cases.<sup>34–37</sup>

The computed dihedral angles of puckering are 35°, 29°, and 31° for the hydride, fluoride, and chloride, respectively, and these values are likely more reliable than the electron diffraction determinations, which average structures over all of the occupied vibrational states. For silacyclobutane the agreement with the far-infrared result (36°) is almost perfect, but the electron diffraction results<sup>6,7,11</sup> of 34°, 25°, and 26°, respectively, agree less well. Since these molecules will have smaller puckering dihedral angles in their higher quantum states of the low-frequency puckering mode, the lower values from the electron diffraction studies are not surprising.

## Vibrational Assignments

Figures 3 to 6 show comparisons of the calculated infrared spectra for the four silacyclobutanes to the experimental vapor-phase infrared spectra previously reported.<sup>12,38</sup> Figures 7 to 10 compare the experimental frequencies and intensities of the Raman spectra with those computed from the B3LYP level of theory. Since published figures for the experimental liquid-phase Raman spectra were not available, the experimental data are represented by vertical bars to reflect their relative intensities. As is evident, the DFT calculations do an outstanding job, one might even say remarkable job, of predicting the spectra and a much better job than any of the MP2 *ab initio* calculations. Tables 5 to 8 present the summary of the assigned frequencies for the four molecules and compare them to the DFT calculations. Whereas most of the previous assignments<sup>12</sup> have been

(30) Foresman, J. B.; Frisch, A. In *Exploring Chemistry with Electronic Structure Methods*, 2nd ed.; Gaussian, Inc.: Pittsburgh, PA, 1996.

(31) Jensen, F. In *Introduction to Computational Chemistry*, 2nd ed.; Wiley, Inc.: New York, 2001.

(32) Young, D. In *Computational Chemistry*, 1st ed.; Wiley, Inc.: New York, 2001.

(33) Cramer, C. J. In *Essentials of Computational Chemistry*, 1st ed.; Wiley, Inc.: New York, 2002.

(34) Autrey, D.; Laane, J. *J. Phys. Chem. A* **2001**, *105*, 6894.

(35) Autrey, D.; Yang, J.; Laane, J. *J. Mol. Struct.* **2003**, *661*, 23.

(36) Autrey, D.; Haller, K.; Laane, J.; Mlynec, C.; Henning, H. *J. Phys. Chem. A* **2004**, *108*, 36.

(37) Al-Saadi, A. A.; Laane, J. *J. Mol. Struct.* **2007**, *830*, 46.

(38) Laane, J. Ph.D. Thesis, Dept. of Chemistry, Massachusetts Institute of Technology, 1967.

Table 6. Vibrational Spectra of Silacyclobutane-1,1-d<sub>2</sub>

						calculated DFT-B3LYP					
						C <sub>s</sub>			C <sub>2v</sub>		
						experimental <sup>a</sup>					
description						IR <sup>b</sup>	Raman <sup>b</sup>		scaled	intensity	dep. ratio
A <sub>1</sub> , A'	<i>v</i> <sub>1</sub> β-CH <sub>2</sub> sym. str.	2935	m	2925 (570)	p				2914	(55,1269)	0.2
	<i>v</i> <sub>2</sub> α-CH <sub>2</sub> sym. str. (i.p.)	2873	m	2857 (70)	p				2933	(75,2087)	0.2
	<i>v</i> <sub>3</sub> SiD <sub>2</sub> sym. str.	1554	vvs	1548 (1000)	p				1545	(100,1000)	0.1
	<i>v</i> <sub>4</sub> α-CH <sub>2</sub> deform. (i.p.)	1422*	m	1416 (89)	d				1442	(4,127)	0.8
	<i>v</i> <sub>5</sub> β-CH <sub>2</sub> deform.	1458*	vw	1450 (53)	d				1475	(1,40)	0.7
	<i>v</i> <sub>6</sub> α-CH <sub>2</sub> wag. (i.p.)	1128	ms	1123 (84)	p				1140	(14,50)	0.2
	<i>v</i> <sub>7</sub> SiD <sub>2</sub> deform.	712	vvs	700 (80)	p				698	(84,27)	0.2
	<i>v</i> <sub>8</sub> C—C sym. str.	867*	m	867* (107)	p				867	(16,119)	0.1
	<i>v</i> <sub>9</sub> Si—C sym. str.	821*	w	819* (58)	p				819	(3,48)	0.0
	<i>v</i> <sub>10</sub> ring deform.	496	mw	499 (204)	p				494	(13,86)	0.3
A <sub>2</sub> , A''	<i>v</i> <sub>11</sub> α-CH <sub>2</sub> antisym. str. (o.p.)	2992*	vs	2980* (260)	d				2992	(20,866)	0.8
	<i>v</i> <sub>12</sub> α-CH <sub>2</sub> twist. (o.p.)								960	(0,4)	0.8
	<i>v</i> <sub>13</sub> β-CH <sub>2</sub> twist.	1216*	vw	1210* (29)	d				1231	(0,62)	0.8
	<i>v</i> <sub>14</sub> α-CH <sub>2</sub> rock. (o.p.)	669*	ms	669* (30)	d				664	(34,19)	0.8
	<i>v</i> <sub>15</sub> SiD <sub>2</sub> twist	410	vvs	417 (78)	d				405	(0,44)	0.8
B <sub>1</sub> , A'	<i>v</i> <sub>16</sub> α-CH <sub>2</sub> sym. str. (o.p.)	2885	ms	2874 (152)	p				2935	(28,150)	0.8
	<i>v</i> <sub>17</sub> α-CH <sub>2</sub> deform. (o.p.)	1404	m						1426	(6,31)	0.8
	<i>v</i> <sub>18</sub> α-CH <sub>2</sub> wag (o.p.)								1074	(1,5)	0.8
	<i>v</i> <sub>19</sub> β-CH <sub>2</sub> wag	1271*	vvs						1277	(0,10)	0.8
	<i>v</i> <sub>20</sub> C—C antisym. str.	925	m	927 (49)	d				925	(9,32)	0.8
B <sub>2</sub> , A''	<i>v</i> <sub>21</sub> Si—C antisym. str.	720*	m	716 (78)	d				715	(53,21)	0.8
	<i>v</i> <sub>22</sub> SiD <sub>2</sub> wag	550*	m	550* (107)	d				537	(18,71)	0.8
	<i>v</i> <sub>23</sub> β-CH <sub>2</sub> antisym. str.	2935*	m	2934* (230)	p				2954	(30,1037)	0.2
	<i>v</i> <sub>24</sub> α-CH <sub>2</sub> antisym. str. (i.p.)	2953	vs						2994	(27,885)	0.4
	<i>v</i> <sub>25</sub> SiD <sub>2</sub> antisym. str.	1566	vvs	1564 (100)	d				1564	(95,428)	0.7
	<i>v</i> <sub>26</sub> α-CH <sub>2</sub> twist. (i.p.)	1193	w	1193 (13)	d				1201	(1,27)	0.4
	<i>v</i> <sub>27</sub> α-CH <sub>2</sub> rock. (i.p.)	902*	ms	898* (209)	p				899	(12,109)	0.1
	<i>v</i> <sub>28</sub> β-CH <sub>2</sub> rock	656	ms	660 (156)	p				650	(9,92)	0.2
	<i>v</i> <sub>29</sub> SiD <sub>2</sub> rock	352	mw	358 (36)	d				347	(6,10)	0.5
	<i>v</i> <sub>30</sub> ring puckering	150 <sup>c</sup>							139	(0,1)	0.4

<sup>a</sup> Reassigned frequencies are labeled with (\*). Frequencies given in *italics* are from ref 38. <sup>b</sup> Vapor-phase experiments from ref 11. <sup>c</sup> Ref. 4.

unchanged, the vibrational representations available from our new calculations have allowed several of the assignments to be modified. The vibrational frequencies of both the C<sub>s</sub> (puckered)

and C<sub>2v</sub> (planar) structures were calculated to aid with the assignments since for the more symmetrical C<sub>2v</sub> structure the vibrations are separated into four separate symmetry blocks.

Table 7. Vibrational Spectra of 1,1-Difluorosilacyclobutane

						calculated DFT-B3LYP					
						C <sub>s</sub>			C <sub>2v</sub>		
						experimental <sup>a</sup>					
description						IR <sup>b</sup>	Raman <sup>b</sup>		scaled	intensity	dep. ratio
A <sub>1</sub> , A'	<i>v</i> <sub>1</sub> β-CH <sub>2</sub> sym. str.	2885*	ms	2883* (92)	p				2939	(20,329)	0.3
	<i>v</i> <sub>2</sub> α-CH <sub>2</sub> sym. str. (i.p.)	2955*	s	2950* (1000)	p				2949	(1,1000)	0.1
	<i>v</i> <sub>3</sub> SiF <sub>2</sub> sym. str.	934*	vs	925* (277)	p				912	(83,46)	0.1
	<i>v</i> <sub>4</sub> α-CH <sub>2</sub> deform. (i.p.)	1400*	ms	1409* (111)	d				1430	(3,46)	0.7
	<i>v</i> <sub>5</sub> β-CH <sub>2</sub> deform.	1460*	ms	1452* (32)	d				1471	(1,13)	0.7
	<i>v</i> <sub>6</sub> α-CH <sub>2</sub> wag. (i.p.)	1135	vs	1135 (25)	p				1144	(38,4)	0.2
	<i>v</i> <sub>7</sub> SiF <sub>2</sub> deform.	293*	m	291* (65)	p				277	(8,3)	0.5
	<i>v</i> <sub>8</sub> C—C sym. str.	862*	s	855* (123)	p				854	(17,22)	0.1
	<i>v</i> <sub>9</sub> Si—C sym. str.	796*	ms	797* (138)	p				790	(29,25)	0.1
	<i>v</i> <sub>10</sub> ring deform.	489*	s	488* (315)	p				478	(10,24)	0.1
A <sub>2</sub> , A''	<i>v</i> <sub>11</sub> α-CH <sub>2</sub> antisym. str. (o.p.)								3004	(4,411)	0.8
	<i>v</i> <sub>12</sub> α-CH <sub>2</sub> twist. (o.p.)								945	(0,0)	0.8
	<i>v</i> <sub>13</sub> β-CH <sub>2</sub> twist.	1222*	w [sol.]	1222* (42)	d				1230	(1,14)	0.8
	<i>v</i> <sub>14</sub> α-CH <sub>2</sub> rock. (o.p.)								620	(0,0)	0.8
	<i>v</i> <sub>15</sub> SiF <sub>2</sub> twist			203 (54)	d				182	(0,4)	0.8
B <sub>1</sub> , A'	<i>v</i> <sub>16</sub> α-CH <sub>2</sub> sym. str. (o.p.)	2850*	m [sol.]						2948	(8,46)	0.8
	<i>v</i> <sub>17</sub> α-CH <sub>2</sub> deform. (o.p.)								1418	(9,8)	0.8
	<i>v</i> <sub>18</sub> α-CH <sub>2</sub> wag (o.p.)			1064* (19)	d				1075	(0,7)	0.8
	<i>v</i> <sub>19</sub> β-CH <sub>2</sub> wag	1242*	w						1266	(1,3)	0.8
	<i>v</i> <sub>20</sub> C—C antisym. str.	913	m	912 (92)	d				908	(11,13)	0.8
B <sub>2</sub> , A''	<i>v</i> <sub>21</sub> Si—C antisym. str.	742	vs	743 (111)	d				724	(55,11)	0.8
	<i>v</i> <sub>22</sub> SiF <sub>2</sub> wag	328	s	331 (42)	d				314	(17,4)	0.8
	<i>v</i> <sub>23</sub> β-CH <sub>2</sub> antisym. str.	2995	s	2998 (385)	d				2980	(6,339)	0.3
	<i>v</i> <sub>24</sub> α-CH <sub>2</sub> antisym. str. (i.p.)	2970	mw [liq.]	2970 (77)	?				3008	(12,242)	0.5
	<i>v</i> <sub>25</sub> SiF <sub>2</sub> antisym. str.	962	vs	945 vw	?				940	(100,4)	0.1
	<i>v</i> <sub>26</sub> α-CH <sub>2</sub> twist. (i.p.)	1185		1184 (42)	d				1192	(3,9)	0.6
	<i>v</i> <sub>27</sub> α-CH <sub>2</sub> rock. (i.p.)	805		809(100)	?				810	(23,17)	0.2
	<i>v</i> <sub>28</sub> β-CH <sub>2</sub> rock	665		666 (38)	p				660	(2,16)	0.1
	<i>v</i> <sub>29</sub> SiF <sub>2</sub> rock	228*		229* (12)	d				215	(1,2)	0.7
	<i>v</i> <sub>30</sub> ring puckering	63 <sup>c</sup>							77	(0,1)	<i>i</i>

<sup>a</sup> Reassigned frequencies are labeled with (\*). Frequencies given in *italics* are from ref 38. <sup>b</sup> Vapor-phase experiments from ref 12. [sol.] = solid state, [liq.] = liquid phase. <sup>c</sup> Ref 4.



**Table 8. Vibrational Spectra of 1,1-Dichlorosilacyclobutane**

description		calculated DFT-B3LYP									
		experimental <sup>a</sup>				C <sub>s</sub>			C <sub>2v</sub>		
		IR <sup>b</sup>		Raman <sup>b</sup>		scaled	intensity	dep. ratio	scaled	intensity	dep. ratio
A <sub>1</sub> , A'	<i>v</i> <sub>1</sub> β-CH <sub>2</sub> sym. str.	2952	ms	2941 (748)	p	2936	(20,690)	0.1	2942	(21,536)	0.0
	<i>v</i> <sub>2</sub> α-CH <sub>2</sub> sym. str. (i.p.)	2887	mw	2878 (141)	p	2948	(1,1282)	0.3	2960	(2,1512)	0.3
	<i>v</i> <sub>3</sub> SiCl <sub>2</sub> sym. str.	376	m	379 (1000)	p	364	(3,100)	0.1	365	(4,100)	0.1
	<i>v</i> <sub>4</sub> α-CH <sub>2</sub> deform. (i.p.)	1414*	mw	1410* (115)	d	1433	(3,67)	0.7	1427	(2,79)	0.7
	<i>v</i> <sub>5</sub> β-CH <sub>2</sub> deform.	1463*	w	1452* (31)	d	1472	(1,18)	0.7	1469	(0,13)	0.7
	<i>v</i> <sub>6</sub> α-CH <sub>2</sub> wag. (i.p.)	1130	ms	1127 (66)	p	1141	(16,18)	0.2	1139	(18,15)	0.1
	<i>v</i> <sub>7</sub> SiCl <sub>2</sub> deform.	168	w	167 (44)	d	165	(2,14)	0.8	164	(2,15)	0.7
	<i>v</i> <sub>8</sub> C–C sym. str.	893	m	893 (243)	p	890	(16,70)	0.1	873	(5,104)	0.1
	<i>v</i> <sub>9</sub> Si–C sym. str.	824*	w	826* (54)	p	817	(7,23)	0.1	783	(10,46)	0.1
	<i>v</i> <sub>10</sub> ring deform.	601	vs	592 (51)	p	583	(100,12)	0.2	585	(100,7)	0.0
A <sub>2</sub> , A''	<i>v</i> <sub>11</sub> α-CH <sub>2</sub> antisym. str. (o.p.)	2952	ms	2952 (50)	?	3010	(4,492)	0.8	3004	(0,677)	0.8
	<i>v</i> <sub>12</sub> α-CH <sub>2</sub> twist. (o.p.)					946	(0,0)	0.8	953	(0,0)	0.8
	<i>v</i> <sub>13</sub> β-CH <sub>2</sub> twist.	1212*	w	1211* (41)	d	1226	(0,30)	0.8	1233	(0,21)	0.8
	<i>v</i> <sub>14</sub> α-CH <sub>2</sub> rock. (o.p.)	653*	m			633	(2,0)	0.8	623	(0,0)	0.8
	<i>v</i> <sub>15</sub> SiCl <sub>2</sub> twist	174	mw	177 (130)	d	154	(0,10)	0.8	153	(0,11)	0.8
	<i>v</i> <sub>16</sub> α-CH <sub>2</sub> sym. str. (o.p.)	2891	mw			2947	(7,117)	0.8	2957	(10,64)	0.8
B <sub>1</sub> , A'	<i>v</i> <sub>17</sub> α-CH <sub>2</sub> deform. (o.p.)	1395	m	1385 (12)	d	1419	(9,16)	0.8	1418	(12,4)	0.8
	<i>v</i> <sub>18</sub> α-CH <sub>2</sub> wag (o.p.)					1071	(0,4)	0.8	1093	(0,0)	0.8
	<i>v</i> <sub>19</sub> β-CH <sub>2</sub> wag	1260*	vw	1248* (11)	?	1271	(0,7)	0.8	1261	(0,14)	0.8
	<i>v</i> <sub>20</sub> C–C antisym. str.	914	m	914 (12)	d	915	(4,11)	0.8	916	(4,10)	0.8
	<i>v</i> <sub>21</sub> Si–C antisym. str.	723	s	725 (123)	d	704	(25,22)	0.8	702	(31,23)	0.8
	<i>v</i> <sub>22</sub> SiCl <sub>2</sub> wag	240*	mw	241* (49)	d	231	(5,1)	0.8	231	(5,11)	0.8
	<i>v</i> <sub>23</sub> β-CH <sub>2</sub> antisym. str.	2972*	m	2972* (175)	p?	2979	(7,516)	0.4	2980	(3,197)	0.8
	<i>v</i> <sub>24</sub> α-CH <sub>2</sub> antisym. str. (i.p.)	3002*	m	2999* (379)	p	3011	(7,431)	0.5	3010	(12,277)	0.8
	<i>v</i> <sub>25</sub> SiCl <sub>2</sub> antisym. str.	533	s	523 (71)	p	509	(56,24)	0.5	517	(80,23)	0.8
	<i>v</i> <sub>26</sub> α-CH <sub>2</sub> twist. (i.p.)	1183	w	1181 (13)	p	1190	(2,11)	0.4	1181	(3,8)	0.8
B <sub>2</sub> , A''	<i>v</i> <sub>27</sub> α-CH <sub>2</sub> rock. (i.p.)	857*	s	863* (32)	p	860	(27,47)	0.1	854	(48,1)	0.8
	<i>v</i> <sub>28</sub> β-CH <sub>2</sub> rock	696*	s	693* (18)	d	687	(46,11)	0.2	705	(28,1)	0.8
	<i>v</i> <sub>29</sub> SiCl <sub>2</sub> rock			212* (18)	d	208	(1,9)	0.7	168	(1,14)	0.8
	<i>v</i> <sub>30</sub> ring puckering					81	(0,7)	0.7	<i>i</i>		

<sup>a</sup> Reassigned frequencies are labeled with (\*). <sup>b</sup> Vapor-phase experiments from ref 12.**Table 9. Vibrational Frequencies of the SiX<sub>2</sub> Group**

vibration	molecule	X = H	X = D	X = F	X = Cl
antisym. stretch	SCB	2145	1566	962	533
	3SCP	2158	1577	947	588
	DSCP	2157, 2155	1579, 1576		
sym. stretch	SCB	2145	1554	934	376 <sup>a</sup>
	3SCP	2155	1564	888	356 <sup>a</sup>
	DSCP	2155, 2147	1554, 1554		
deformation	SCB	962	715	293	168
	3SCP	960	718	276 <sup>b</sup>	170
	DSCP	965, 928	695, 692		
wag	SCB	814 <sup>a</sup>	550 <sup>a</sup>	328	240
	3SCP	861	642	320	230
	DSCP	905, 745	546, 543		
twist	SCB	514	410	203	174
	3SCP	588	436	?	164
	DSCP	555, 442	428, 428		
rock	SCB	409	352	228	212
	3SCP	458	409	200 <sup>b</sup>	208
	DSCP	438, 380	344, 332		

<sup>a</sup> Coupled to ring vibration. <sup>b</sup> Reassigned.

The frequencies calculated for the two conformations of the four molecules are in most cases within 10 cm<sup>-1</sup> of each other. Use of the higher symmetry for the calculations eliminates the possibility of vibrational coupling between vibrations in different *C<sub>2v</sub>* symmetry blocks and greatly helps in recognizing the best assignment for each vibrational mode.

For the characterization of organosilanes it is important to know the vibrational frequencies expected for the six modes associated with each SiX<sub>2</sub> group. Table 9 compares the data from the present work for the silacyclobutanes (SCB) to those

**Table 10. Atomic Charges for Silacyclobutane, 1,1-Difluorosilacyclobutane, and 1,1-Dichlorosilacyclobutane as Predicted from the DFT-B3LYP/cc-pVTZ Level of Theory<sup>a</sup>**

	silacyclobutane (X = H)	1,1-difluoro- silacyclobutane (X = F)	1,1-dichloro- silacyclobutane (X = Cl)
Si	0.27	0.77	0.59
X <sub>a</sub>	-0.05	-0.29	-0.24
X <sub>b</sub>	-0.05	-0.29	-0.24
C <sub>α</sub>	-0.29	-0.32	-0.29
H <sub>a</sub> (C <sub>α</sub> )	0.10	0.11	0.11
H <sub>b</sub> (C <sub>α</sub> )	0.10	0.10	0.10
C <sub>β</sub>	-0.16	-0.17	-0.17
H <sub>a</sub> (C <sub>β</sub> )	0.09	0.10	0.11
H <sub>b</sub> (C <sub>β</sub> )	0.09	0.10	0.11

<sup>a</sup> See Figure 1 for atom labels.

of 1,3-disilacyclobutanes (DSCB)<sup>27,39</sup> and 3-silacyclopentene (3SCP).<sup>40</sup> As can be seen, the functional group frequency associated with each type of vibration is in a narrow range for the Si–H and Si–D stretches but covers a broader wavenumber range for the lower frequency vibrations. This is to a small extent due to the bonding differences in the three molecules, but it arises mostly from the coupling of the SiX<sub>2</sub> modes with other vibrations of the molecules. For example, the SiCl<sub>2</sub> symmetric stretching frequencies of both the chlorides of SCB and 3SCP are significantly pushed down from their expected values<sup>13,14</sup> near 450 cm<sup>-1</sup> by their interactions with ring-bending modes, which in turn are pushed up to higher values. The DFT calculations in our present study very nicely confirm that. For the SCB with X = Cl the strongest Raman band at 379 cm<sup>-1</sup> along with the very strong infrared band at 601 cm<sup>-1</sup> both result from the combination of the SiCl<sub>2</sub> symmetric stretching with the lowest frequency ring-bending motion. Similarly, the SiH<sub>2</sub>

(39) Irwin, R. M.; Laane, J. *J. Phys. Chem.* **1978**, 82, 2845.(40) Chao, T. H.; Laane, J. *Spectrochim. Acta* **1972**, 28A, 2443.

and the SiD<sub>2</sub> wagging modes for SCB and its d<sub>2</sub> isotopomer have been shifted down by interactions with ring stretching modes. Nonetheless, Table 9 provides some useful guidelines for where to expect these SiX<sub>2</sub> vibrational frequencies for X = H, D, F, and Cl.

A valuable finding<sup>3,12</sup> in the study of silacyclobutanes was that this ring system always gives rise to an infrared band of at least moderate intensity near 1130 cm<sup>-1</sup>, and thus it is considered an identifier of this ring system. As can be seen in Tables 5 to 8, this band is between 1127 and 1135 cm<sup>-1</sup> in the four molecules investigated in this study, and it has at least a medium strong intensity. The DFT calculation carried out predicts both the wavenumber and intensity of this vibration very well and shows that the motion is indeed the α-CH<sub>2</sub> in-phase wagging of the methylene groups next to the silicon atom. The intensity of this band is clearly enhanced by the presence of the adjacent electropositive silicon atom and leads to a substantial dipole moment change for this motion. The β-CH<sub>2</sub> wag, on the other hand, has much lower infrared intensity. The α-CH<sub>2</sub> in-phase wagging motion is also somewhat coupled to the symmetric stretching of the Si–C and C–C bonds in the ring, and this further enhances its infrared absorption intensity.

One unexpected result from our DFT calculations was the discovery that the frequencies of the out-of-phase CH<sub>2</sub> twisting (ν<sub>12</sub>) and the out-of-phase CH<sub>2</sub> wagging (ν<sub>18</sub>) vibrations are much lower than the original assignments,<sup>12</sup> which were based on expected values.<sup>41</sup> These two A<sub>2</sub> vibrations are calculated to have the weakest infrared intensities among the fundamentals for the four molecules and thus were difficult to assign without the DFT calculations. Several other studies<sup>42–47</sup> have employed DFT calculations to predict vibrational frequencies and to compare them with previous experimental results for some noncyclic silicon-containing molecules including dimethylsilane,<sup>44,46</sup> trimethylsilane,<sup>43,46</sup> disilylmethane,<sup>45,47</sup> and ethylsilane.<sup>42</sup> These studies utilized the calculated frequencies to reinvestigate some of the uncertain aspects of the vibrational spectra recorded many years earlier, but none of these studies noted why such a discrepancy between the experimental and calculated frequencies for these CH<sub>2</sub> out-of-phase modes should occur.<sup>42–47</sup> Nevertheless, one conclusion drawn from all these studies as well as our own is that the presence of a silicon atom in the structure of a molecule does not adversely affect the accuracy of the vibrational frequencies calculated by the DFT method. Moreover, for disilylmethane (CH<sub>3</sub>SiH<sub>2</sub>CH<sub>3</sub>), the CH<sub>2</sub> twisting vibration was previously predicted with the B3LYP/6-311G(d,p) level of theory<sup>45</sup> to be at 1043 cm<sup>-1</sup>, which is at a somewhat lower value than had been assigned before<sup>47</sup> (1101 cm<sup>-1</sup>).

Our recent *ab initio* and DFT study on 1,3-disilacyclobutane (DSCB)<sup>27</sup> suggested that there is an electrostatic interaction

between the partially negatively charged hydrogen atoms on the electropositive silicon atoms and the electropositive hydrogen atoms of the CH<sub>2</sub> groups. The attractive interaction between the two types of hydrogen atoms causes the CH<sub>2</sub> out-of-phase frequencies to be shifted to lower frequencies below 1000 cm<sup>-1</sup> since the force constant governing the motion is reduced. In SCB, as shown in Table 5, the out-of-phase CH<sub>2</sub> twisting (ν<sub>12</sub>) and the out-of-phase CH<sub>2</sub> wagging (ν<sub>18</sub>) frequencies were calculated to be 969 and 1074 cm<sup>-1</sup>, respectively, which are considerably lower than typical values (1100–1300 cm<sup>-1</sup>) for these motions. For the difluoro and dichloro derivatives (Tables 7 and 8), the frequency of the ν<sub>12</sub> mode was calculated to be even lower (946 cm<sup>-1</sup>). This is clearly due to the larger partial negative charges on the halogen atoms, which give rise to greater attractive interaction and reduce the wagging force constants even more. Table 10 presents the atomic charges calculated for the individual atoms in this work. This clearly shows the electropositive nature of the hydrogen atoms on the α-carbon atoms as well as the electronegative character of the X atoms of the SiX<sub>2</sub> groups. The fluorine and chlorine atoms can be seen to have especially large negative charges (–0.29 and –0.24, respectively).

## Conclusion

In this work we have utilized high-level *ab initio* calculations to compute the structure of silacyclobutane and its two halo derivatives, and we have shown that this provides accurate structures for these molecules. The reliability of such computations is well known for typical organic compounds, but there has been concern that *ab initio* studies on larger molecules such as organosilanes may not be as reliable. The results of these calculations have confirmed the experimental structures for these molecules and have allowed us to understand structural changes resulting from the electronegative halogen atoms. The high-level triple-ζ calculation also reliably predicts the rotational constants and the puckering angle of the silacyclobutane and does an excellent job in reproducing the experimental potential energy function. We have also utilized high-level density functional theory (DFT) to compute the infrared and Raman spectra of each of these molecules and have found an extremely good agreement with the observed spectra. The DFT calculations have allowed several of the observed infrared and Raman bands to be reassigned. These include the out-of-phase CH<sub>2</sub> twisting and the out-of-phase CH<sub>2</sub> wagging modes, whose frequencies are lowered by the electrostatic attraction between the wagging hydrogen atoms and the X atoms on the adjacent SiX<sub>2</sub> groups. The DFT calculations have also confirmed the nature of the characteristic infrared band near 1130 cm<sup>-1</sup> present in all silacyclobutanes and arising from the α-CH<sub>2</sub> in-phase wagging. Finally, it can be noted that our calculations have also allowed us to provide reliable frequency ranges expected for the six vibrations of each SiX<sub>2</sub> group.

**Acknowledgment.** The authors wish to thank the National Science Foundation (Grant CHE-0131935) and the Robert A. Welch Foundation (Grant A-0396) for financial support. A.A.-S. also thanks King Fahd University of Petroleum and Minerals (KFUPM) for its financial support.

OM800296W

(41) Colthup, N. B. In *Introduction to Infrared and Raman Spectroscopy*, 2nd ed.; Academic Press: New York, 1975.

(42) Mohamed, T. A.; Guirgis, G. A.; Nashed, Y. E.; Durig, J. R. *Struct. Chem.* **1998**, *9*, 255.

(43) McKean, D. C. *Spectrochim. Acta* **1999**, *55A*, 1485.

(44) McKean, D. C.; Torto, I. J. *Mol. Spectrosc.* **2002**, *216*, 363.

(45) McKean, D. C. *J. Phys. Chem. A* **2003**, *107*, 6538.

(46) Ball, D. F.; Goggin, P. L.; McKean, D. C.; Woodward, L. A. *Spectrochim. Acta* **1960**, *16*, 1358.

(47) McKean, D. C.; Davidson, G.; Woodward, L. A. *Spectrochim. Acta* **1970**, *26A*, 1815.